NASA/TM—2012-217619

Wear of Steel and Ti6Al4V Rollers in Vacuum

Timothy L. Krantz
Glenn Research Center, Cleveland, Ohio

Iqbal Shareef
SFF Bradley University, Peoria, Illinois

June 2012

NASA STI Program . . . in Profile

Since its founding, NASA has been dedicated to the advancement of aeronautics and space science. The NASA Scientific and Technical Information (STI) program plays a key part in helping NASA maintain this important role.

The NASA STI Program operates under the auspices of the Agency Chief Information Officer. It collects, organizes, provides for archiving, and disseminates NASA's STI. The NASA STI program provides access to the NASA Aeronautics and Space Database and its public interface, the NASA Technical Reports Server, thus providing one of the largest collections of aeronautical and space science STI in the world. Results are published in both non-NASA channels and by NASA in the NASA STI Report Series, which includes the following report types:

- TECHNICAL PUBLICATION. Reports of completed research or a major significant phase of research that present the results of NASA programs and include extensive data or theoretical analysis. Includes compilations of significant scientific and technical data and information deemed to be of continuing reference value. NASA counterpart of peer-reviewed formal professional papers but has less stringent limitations on manuscript length and extent of graphic presentations.

- TECHNICAL MEMORANDUM. Scientific and technical findings that are preliminary or of specialized interest, e.g., quick release reports, working papers, and bibliographies that contain minimal annotation. Does not contain extensive analysis.

- CONTRACTOR REPORT. Scientific and technical findings by NASA-sponsored contractors and grantees.

- CONFERENCE PUBLICATION. Collected papers from scientific and technical conferences, symposia, seminars, or other meetings sponsored or cosponsored by NASA.

- SPECIAL PUBLICATION. Scientific, technical, or historical information from NASA programs, projects, and missions, often concerned with subjects having substantial public interest.

- TECHNICAL TRANSLATION. English-language translations of foreign scientific and technical material pertinent to NASA's mission.

Specialized services also include creating custom thesauri, building customized databases, organizing and publishing research results.

For more information about the NASA STI program, see the following:

- Access the NASA STI program home page at *http://www.sti.nasa.gov*

- E-mail your question to *help@sti.nasa.gov*

- Fax your question to the NASA STI Information Desk at 443–757–5803

- Phone the NASA STI Information Desk at 443–757–5802

- Write to:
  STI Information Desk
  NASA Center for AeroSpace Information
  7115 Standard Drive
  Hanover, MD 21076–1320

NASA/TM—2012-217619

Wear of Steel and Ti6Al4V Rollers in Vacuum

Timothy L. Krantz
Glenn Research Center, Cleveland, Ohio

Iqbal Shareef
SFF Bradley University, Peoria, Illinois

Prepared for the
41st Aerospace Mechanisms Symposium
cosponsored by the NASA Jet Propulsion Laboratory and Lockeed Martin Space Systems Company
Pasadena, California, May 16–18, 2012

National Aeronautics and
Space Administration

Glenn Research Center
Cleveland, Ohio 44135

June 2012

Acknowledgments

This research was supported by the NASA Engineering Safety Center. The experimental work was done with assistance from Mr. Richard Manco, Sierra Lobo Inc. Dr. Iqbal Shareef's contributions were supported by the NASA GRC Summer Faculty Fellowship Program.

This report contains preliminary findings, subject to revision as analysis proceeds.

Level of Review: This material has been technically reviewed by technical management.

Available from

NASA Center for Aerospace Information
7115 Standard Drive
Hanover, MD 21076–1320

National Technical Information Service
5301 Shawnee Road
Alexandria, VA 22312

Available electronically at http://www.sti.nasa.gov

Wear of Steel and Ti6Al4V Rollers in Vacuum

Timothy L. Krantz
National Aeronautics and Space Administration
Glenn Research Center
Cleveland, Ohio 44135

Iqbal Shareef
SFF Bradley University
Peoria, Illinois 61625

Abstract

This investigation was prompted by results of a qualification test of a mechanism to be used for the James Webb Space Telescope. Post-test inspections of the qualification test article revealed some loose wear debris and wear of the steel rollers and the mating Ti6Al4V surfaces. An engineering assessment of the design and observations from the tested qualification unit suggested that roller misalignment was a controlling factor. The wear phenomena were investigated using dedicated laboratory experiments. Tests were done using a vacuum roller rig for a range of roller misalignment angles. The wear in these tests was mainly adhesive wear. The measured wear rates were highly correlated to the misalignment angle. For all tests with some roller misalignment, the steel rollers lost mass while the titanium rollers gained mass indicating strong adhesion of the steel with the titanium alloy. Inspection of the rollers revealed that the adhesive wear was a two-way process as titanium alloy was found on the steel rollers and vice versa. The qualification test unit made use of 440F steel rollers in the annealed condition. Both annealed 440F steel rollers and hardened 440C rollers were tested in the vacuum roller rig to investigate possibility to reduce wear rates and the risk of loose debris formation. The 440F and 440C rollers had differing wear behaviors with significantly lesser wear rates for the 440C. For the test condition of zero roller misalignment, the adhesive wear rates were very low, but still some loose debris was formed.

Introduction

This investigation was prompted by results of a qualification test of a mechanism to be used for the James Webb Space Telescope. The mechanism is used to move a magnet for certain operations of the telescope's near infrared spectrometer (NIRSpec) instrument. The motion of the magnet is guided by a set of preloaded steel rollers in contact with anodized Ti6Al4V. The qualification testing was accomplished in a cold vacuum chamber to match as closely as possible the extreme deep space environment. Post-test inspections of the qualification test article revealed some wear of the steel rollers and mating Ti6Al4V surfaces, and some loose debris was found. The NASA Engineering Safety Center (NESC) is investigating the potential risk of the wear and debris toward hindering the full capability of the NIRSpec instrument. This article will discuss the NESC investigation of the wear phenomena including dedicated laboratory experiments.

Qualification Testing Article and Testing Results

The mechanism of interest is a translator assembly that features a set of 11 rollers to guide the motion of a magnet (Fig. 1). The translation of the magnet is used to affect the positions of micro-shutters. A motor and linkages provide the motive force. The translator assembly undergoes oscillatory motion in a straight line. The translating distance is approximately 200 mm on each stroke (total of 400 mm of travel during back and forth motion) and translation time in one direction during qualification testing was 10.5 sec. The qualification test included 96,000 of such forward and return excursions.

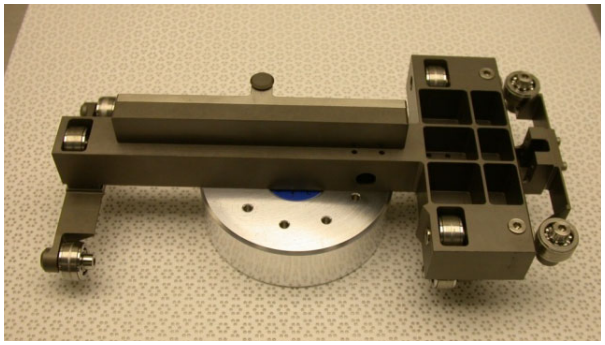

Figure 1.—Translator assembly (Ref. 1).

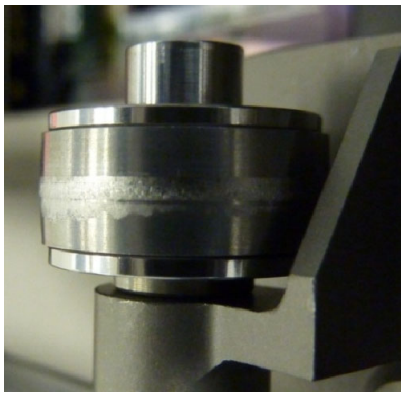

Figure 2.—Condition of roller after completion of qualification test (Ref. 2).

The translator assembly motion is guided by a set of eleven rollers. The in-plane guide is provided by a set of four rollers (two of these rollers are visible to the far right side of Fig. 1). These four rollers contact both sides of a guide rail defining the direction of motion. The out-of-plane position and motion is guided by a set of seven rollers. Three rollers are in contact with a base plate defining one plane and four rollers are in contact with a cover defining a second parallel plane. The roller preloads are set by a shimming procedure to a nominal normal load of about 18 N. The roller is a cylinder with diameter of 21.2 mm. The roller profile is a crown radius with a flat feature in the center of the crown. Assuming line contact across the flat feature, the Hertz contact maximum pressure is about 240 MPa. The rollers are made from 440F steel (a free machining variant of 440C). The roller material was in the annealed condition and passivated. A pair of deep groove ball bearings supports each roller. The fastener securing the roller bearings to the axle is a locking style bolt assembled in a manner allowing for a small amount of axial play. The rollers are in contact with Ti6Al4V that had been stress relieved and anodized.

After completion of the qualification test, wear was visible on the rollers of the translator assembly and on the mating surfaces. Figure 2 shows the condition of a qualification test roller. Some loose particulate debris was also found, which was collected and analyzed (Refs. 1 and 2). The worn surfaces and wear debris provide evidence that the wear process was primarily adhesive wear. In total it appears that the steel has transferred to the mating Ti6Al4V surfaces. The loose wear debris included both the steel and titanium alloy materials. The severity of wear was not the same on all rollers.

From observations of the wear patterns and wear debris of the qualification unit, study of the literature, and engineering assessment of the kinematic configuration, manufacturing tolerances, and roller mounting details, the roller alignment seemed likely to be a key variable influencing the wear rate. To better understand the wear phenomena and to explore possible mitigation strategies, a set of laboratory roller tests were conducted in vacuum. The next sections will discuss the testing apparatus, specimens, procedures, and the corresponding results.

Laboratory Test Apparatus, Specimens, and Procedure

Test Apparatus for Roller Pairs

Testing was done using the NASA Glenn Research Center Vacuum Roller Rig (Fig. 3). The rig allows for application and measurement of a load pressing the rollers together while having a purposely misaligned and adjustable shaft angle. The rig is depicted in schematic form in Figure 4. A drive motor provides motion to the driving roller. A magnetic-particle brake attached to the output shaft imposes torque on the driven roller. The rig can be operated with the brake not energized. For such a condition the torque transmitted through the roller pair is the drag torque of the output shaft (drag of the seals and support bearings). The normal load pressing the rollers together is provided by an air cylinder.

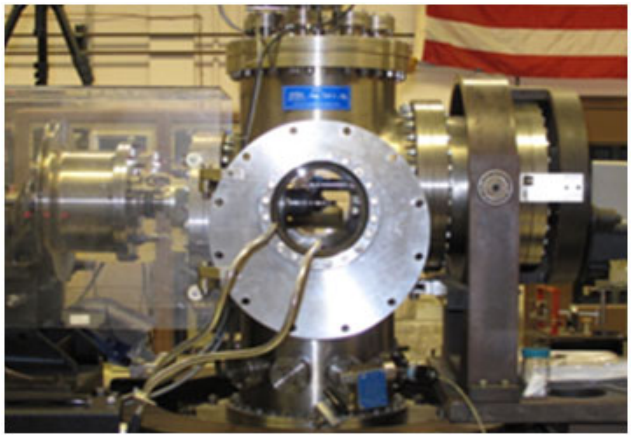

Figure 3.—Vacuum roller rig.

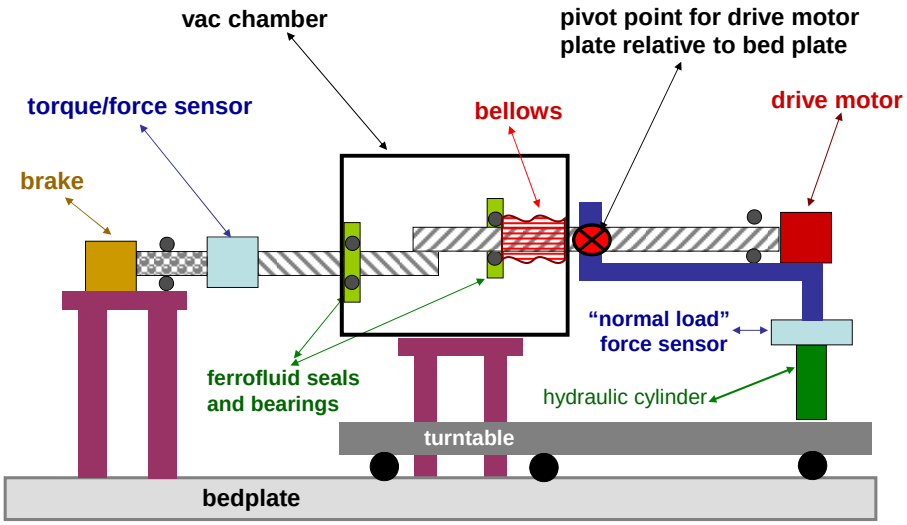

(a)

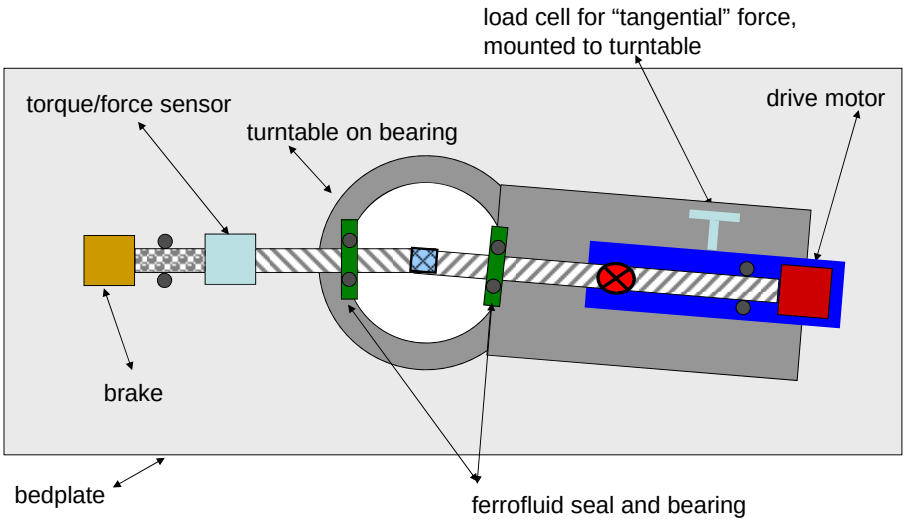

(b)

Figure 4.—Schematic views of the vacuum roller rig. (a) Schematic, side view. (b) Schematic, overhead view with shaft misalignment depicted and exaggerated.

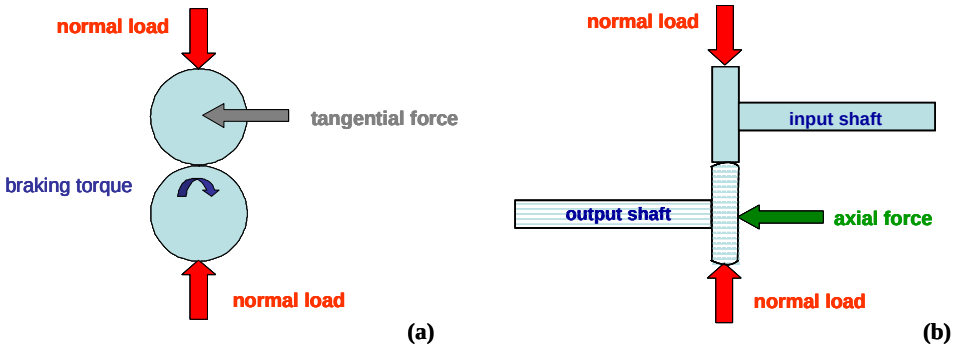

Figure 5.—Simplified schematic view including some of the important sensed data. (a) Schematic, front view. (b) Schematic, side view.

The cylinder acts through a gimbal point to rotate the plate that mounts the driving shaft and drive motor. The rotation of the drive motor plate displaces the driving roller toward the driven roller shaft in an arc motion. The pressure to the cylinder, and thereby the load between the contacting rollers, is adjusted by a hand-operated valve (open-loop control). A turbomolecular pump assisted by a scroll pump provides vacuum in the test chamber. The typical condition in the test chamber is a pressure of about 3×10^{-7} torr. The most prevalent remaining constituent in the chamber during testing is water vapor as determined by residual gas analyzer (Ref. 3). Figure 5 provides a simplified schematic of the test rollers labeled with some of the nomenclature used herein.

A set of sensors on the test apparatus monitors the test conditions. The outputs of the analog sensors were digitized and stored via a data acquisition system at a rate of up to 0.66 Hz. Each of the sensors will be described in turn.

The misalignment of the driving roller shaft and driven roller shaft is depicted in an exaggerated manner in Figure 4(b). The misalignment is measured via a linear variable differential transformer (LVDT). The transducer housing is attached to the bedplate, and the translating, spring-loaded transducer tip contacts against a mechanical stop on the turntable. To establish the aligned condition, special tooling blocks were machined to locate the roller-mounting surfaces of the two shafts as parallel. With the shafts aligned by the tooling blocks, the transducer circuit balance was adjusted to provide an output of zero. The precision of this method for aligning the shafts was limited by the dimensions of the roller mounting surfaces used as the reference planes. From analysis of the test rig drawing tolerances and geometry, the alignment procedure using the tooling blocks to define the zero-degree position has a precision within 0.08°. Rotation of the turntable from the aligned position moves the LVDT sensor. The angular displacement of the turntable was determined by mounting a laser light source on the moving shaft at the roller mounting location and directing the light onto a paper placed at a known radial distance from the center of the turntable. The movement of the laser light was marked on the paper and distance between the points measured and used to relate the sensor output to the angular motion of the turntable.

The torque on the output shaft is monitored by a strain-gage type torquemeter of 22 N-m (200 in.-lb) torque capacity. Calibration was done in place using deadweights acting on a torque arm of known length attached at the test roller position and reacting the output shaft to ground.

The load pressing the rollers together is termed herein the “normal load” (Fig. 5). The normal load is applied via an air-pressure actuated piston. The air piston acts through a load cell against the drive motor plate that is gimbal-mounted relative to the test chamber (Fig. 4(a)). In this way the air piston moves the roller on the input shaft in an arc motion toward the test roller. The arc motion of the input shaft table is measured by an LVDT. Once the rollers are in contact, additional force commanded to the air piston increases the normal load between the test rollers. Careful calibration processes allow calculating the normal load on the test roller based on the sensor outputs from the load cell and the LVDT that measures the input shaft position.

When rollers operate in a misaligned condition a force will develop in the direction of the shaft axis (Refs. 4 to 7). In such a condition points on the two rollers in intimate contact and within a “stick” zone of the contact patch are constrained to move in unison. If the points were not in contact the kinematic constraints would provide a slightly different path of motion. The difference in the actual path of motion and that defined by the motion if the points were not in contact gives rise to surface strains and a resultant axial force. A sensor to measure this force is labeled as the “axial force” sensor in Figure 4. The axial force sensor is co-located on the output shaft with the torquemeter sensor. The configuration of the rig did not allow for direct deadweight calibration in place. To calibrate the sensor in place, the following procedure was used. First, a load cell was calibrated via deadweights and then was placed on the free end of the output shaft to act as a reference load cell. A threaded jackscrew acted against the reference load cell and a hard stop in the vacuum chamber. Adjusting the jackscrew length allowed for changing the force imparted on both the reference load cell and the rig’s axial load cell and to the machine frame. In this manner the same force was applied to both load cells, and the reference cell output was used to calibrate the axial load cell sensor in place.

The preceding two paragraphs describe the sensors (and sensor calibrations) to determine two mutually perpendicular forces acting on the driven test roller. A force also acts along a third axis. This is the force directed tangential to the roller diameter and is termed here as the “tangential” force. The tangential force on the input shaft roller acts through a gimbal point (Fig. 4(b)). The rotational motion about the gimbal point is restrained by a mechanical link to the turntable structure. A load cell is used to sense the force in said mechanical link to the turntable structure. This sensor was calibrated in place by using a pulley-cable system and dead weights to relate the tangential force applied at the test roller position to the sensor output. During testing, this sensor is also affected by spin moments (Refs. 4 and 5) that can develop in roller contacts. The data from the tangential force sensor was recorded for possible future use, but such data were not of immediate interest and are not reported herein.

Shaft speeds and total number of shaft revolutions were measured using encoders on each shaft. The encoder pulses were counted and recorded via a digital pulse counter. The encoder pulses were also monitored by a frequency converter to provide a convenient shaft speed display to the test operator. The encoders provide 6,000 pulses for each shaft revolution.

Test roller conditions were photographed at regular intervals through a viewport. The images were captured digitally using a single-lens reflex camera with a 150 mm micro lens and a 12 million effective pixel image sensor. A debris pan was used to capture debris created from the roller pairs. A video camera recorded the condition of a portion of the debris pan. In spite of several attempts to adjust video camera setting and lighting, the video images failed to capture all that could be observed by eye through the viewport.

Test Specimens

The test specimens used for this research had a nominal geometry of 35.6 mm outer diameter and a 12.7 mm width. The apparatus requires that at least one roller has a crowned profile to avoid edge loading. The roller on the drive motor (input) shaft was provided a crown radius of 200 mm and was made from steel. The roller on the lower (output) shaft had a flat profile and was made from Ti6Al4V alloy.

The material condition, manufacturing details, and surface roughness can all influence the wear behavior. The details of the roller conditions are given in Table I and additional details follow. The qualification test unit has rollers made from 440F steel in the annealed condition and the working surface specified to have a roughness of 0.4 μm maximum. The qualification test rollers were passivated per ASTM A-380-06. The 440F alloy is similar to 440C but includes the introduction of either selenium and/or additional sulfur to alter the machining characteristics relative to 440C. From x-ray photoelectron spectroscopy both the qualification test unit rollers and the 440F laboratory test rollers were found to have selenium as a constituent. The surface hardness of a 440F laboratory test roller was measured as 24 RC. Laboratory test rollers were made intending to enhance resistance to adhesive wear and to reduce debris generation. These rollers were made from 440C, hardened to RC 58, and provided a fine ground surface.

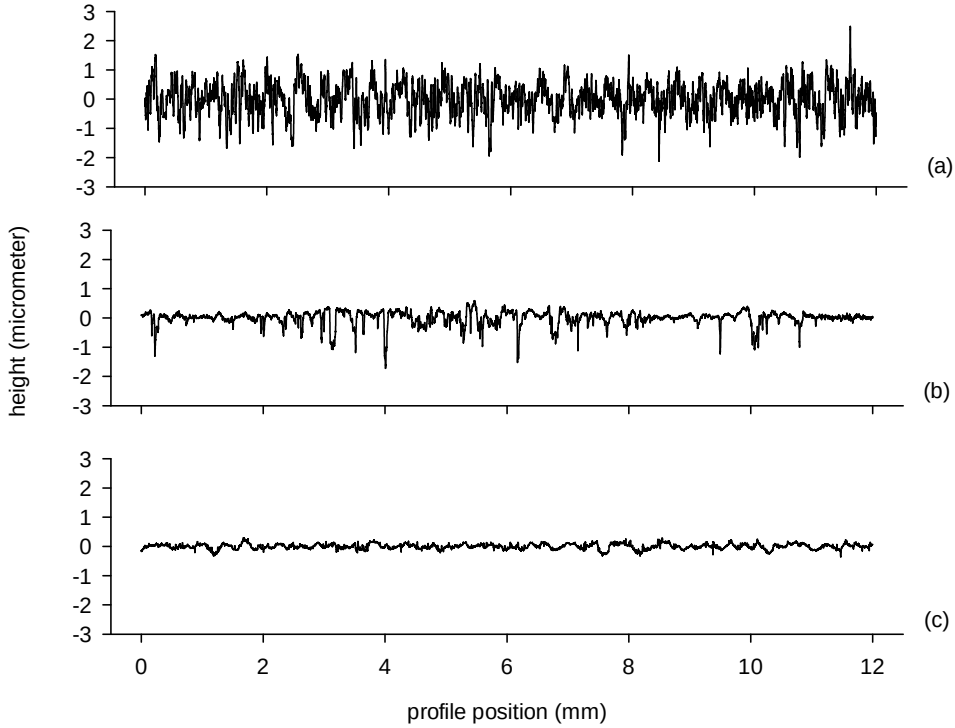

Figure 6.—Typical surface roughness of test rollers, profile traces obtained using a 2-μm radius tip conisphere stylus tracing in the direction of rolling. (a) Ti6Al4V roller. (b) 440F roller. (c) 440C rollers.

Roughness of the test rollers was documented by stylus profilometer inspections. Typical roughness profiles in the rolling direction are provided in Figure 6. The roughness data of Figure 6 were prepared filtering the data using 0.8 mm cutoff and 300:1 bandwidth ISO standard filter. The roughness of the 440F rollers (0.15 μm Ra) was significantly larger than the roughness of the 440C rollers (0.07 μm Ra).

The test rollers that mated with the 440 series rollers were made of Ti6Al4V. The Ti6Al4V rolling surfaces of the qualification unit were observed to have distinctive machining marks, and so the laboratory Ti6Al4V rollers were made using a turning operation as the resulting surface texture of the test rollers were judged similar to the surfaces of the qualification unit. The rollers were stress relieved per AMS 2801 after machining. The roller hardness was RC 35. Some of the Ti6Al4V rollers were anodized per Tifin 200 matching the qualification unit treatment. A typical roughness profile for the Ti6Al4V rollers after anodizing is provided in Figure 6. The typical roughness average value was 0.44 μm Ra. Some testing was done with Ti6Al4V rollers that were not anodized to make project progress previous to the completion of the anodize process.

Procedure to Install Test Rollers

Test specimens were cleaned and installed using careful procedures to provide clean test surfaces. The test rollers were cleaned just prior to installation into the rig using de-ionized water and 0.05 μm alumina powder. After appropriate hand scrubbing, the cleaning powder was rinsed with deionizer water making sure that the entire roller surface wetted uniformly to confirm complete cleaning of surface oils. The water was removed from the roller using dried pressurized nitrogen. Test rollers and mounting hardware were handled only with gloved hands and clean tools to complete installation into the test apparatus.

Procedure for Testing Rollers

The first step for testing after installation of the test rollers was to immediately isolate the testing chamber and provide a vacuum, using the scroll roughing pump, to approximately 50×10^{-3} torr chamber pressure. This isolation step was done even if test scheduling required some delay between the time of installation of rollers and the time for testing to minimize exposure of the cleaned surfaces to any contaminants that might be present in the atmosphere. Prior to testing the turbomolecular pump was used to bring the testing chamber to approximately 3×10^{-7} torr.

Contact analyses were completed to select roller normal loads, speeds, and alignment angle and to relate those choices to the operating conditions of the qualification test unit rollers. The contact conditions for the qualification test were studied assuming that the contact pressure distribution was affected by the moment produced by the axial load caused by misalignment. To estimate this effect, it was assumed that the ratio of axial load to normal load was 0.6 and such load produced an overturning moment by acting through the ball bearing center. It was also assumed that the supporting structure provided 90 percent of the reaction to the overturning moment while the pressure distribution provided 10 percent of the reaction. The pressure distribution for such a loading condition while accounting for the roller profile having a crown but modified with a flat section was calculated using the method of Vijayakar (Refs. 9 and 10). The contact condition for a perfectly aligned roller having zero axial force was also solved. The predicted contact pressure distributions are provided in Figure 7. The misalignment of the roller axis will cause a shift of the pressure from the central flat section onto the crowned region, and a maximum contact pressure of about 450 MPa occurs near the transition from flat to crown geometry. Because of test rig limitations, the laboratory test conditions could not match these conditions exactly. The laboratory testing was done at maximum contact pressure of about 640 MPa. The laboratory tests were used to study trends and fundamental qualitative wear behavior.

The test rig speed was selected using the idea that the “contact time” of the test unit and laboratory rollers should be matched. Here the “contact time” is the time required for a point on the roller to pass through the Hertz contact region. The contact time on the qualification test unit for condition of misaligned rollers was 0.015 sec. To match this condition the test rig was operated at 1.6 rad/s (15 rpm) for the majority of laboratory testing.

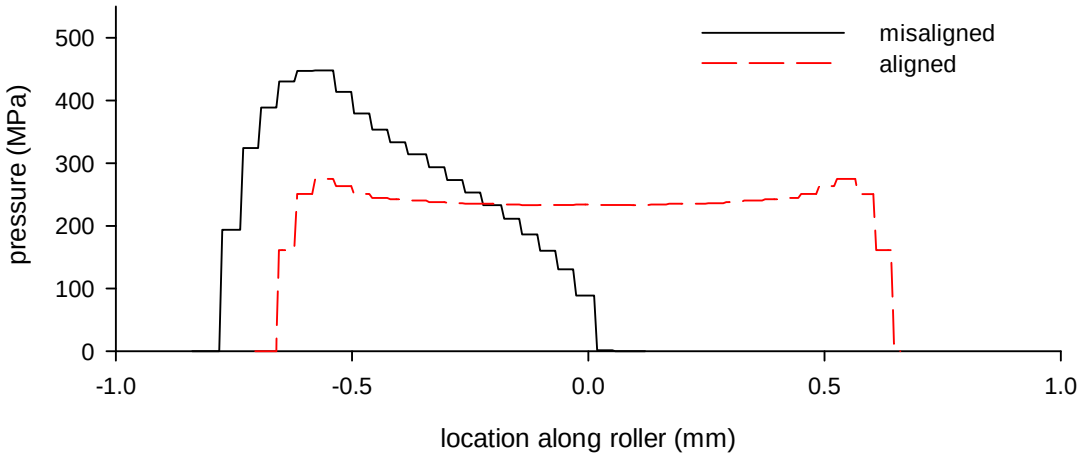

Figure 7.—Contact pressures on qualification test unit roller for cases of misaligned and aligned rollers. The pressures shown are at the midpoint of the Hertz contact in the direction of rolling.

The lab apparatus can be operated with the misalignment angle at a maximum value of about 1.5°. The influence of the misalignment angle on the contact conditions depends on overall system stiffness and the contact dimensions. The sliding distance in such a condition can be approximately quantified as proportional to the product of the misalignment angle and the length of the contact patch in the rolling direction. Using this concept the misalignment angle of the lab test apparatus times a factor of 1.7 provides the approximate simulated misalignment angle of the qualification test unit. The lab test was conducted for misalignment angles up to 1.5° that would simulate a misalignment angle of about 2.5° for the qualification unit.

A summary of the test conditions is provided in Table 1. The tests are listed sequentially in the order of testing. In general one would prefer to have a randomly chosen testing order, but in this work roller availability dictated the testing sequence. In some cases the same roller pair was tested at more than one misalignment angle. In those cases the angles were tested sequencing from smallest to largest.

Post-test documentation of the rollers included recording of the mass of each roller, profilometry, and photographs. Some rollers were inspected via scanning electron microscope. Debris was collected. In some cases the debris was swept from the debris tray, collected to a glass vial, and total mass of debris determined. In some cases debris was collected using a square piece of tacky material that could be placed onto the tray and lifted to collect the debris. The collected debris could then be subjected to automated analysis of debris particle counts and sizes. At completion of one test there was no debris readily visible on the brass-hued debris tray, but a swiping of the tray with a cotton-gloved finger revealed debris. The glove fingertip was saved to retain the debris. For later tests a dark grey anodized plate was used for the debris tray. The darker and matte-finished plate allowed to more easily see the small particles.

Test Results

Roller Wear

Photographs of the test rollers were recorded through a view port during test operations at regular intervals. Figure 8 provides a set of photographs documenting the progression of wear during tests with test ID 3, 4 and 8 (test ID per Table 1). These photos show the difference in wear resulting from material condition. The first two rows of Figure 8 can be used to compare and contrast the wear when using annealed 440F rollers (first row) to the wear when using hardened 440C (second row). In these photos the upper roller is the one made from steel alloy and the lower roller is the titanium alloy. The steel rollers took on a relatively uniform appearance of wear while the titanium rollers had patches of irregular appearance. The wear rate can be qualitatively judged by the width of the wear track of the upper roller that, when new, had a circular crown. As this roller loses material the wear track widens. The worn 440C roller appears slightly smoother than the 440F roller suggesting that steel wear debris would in general be smaller for the case of 440C compared to 440F. Recall that the 440F is alloyed to be “free machining” and to thereby produce chips more easily and of greater length during machining. The last row of Figure 8 shows dramatically reduced wear when the rollers are exactly aligned (final row of Figure 8). Even after significantly longer running time the aligned rollers appear almost like the running-in condition (first few hundred cycles) of the misaligned rollers. Still, for the aligned condition one can notice in the very center of the wear track a narrow band that exhibits adhesive wear.

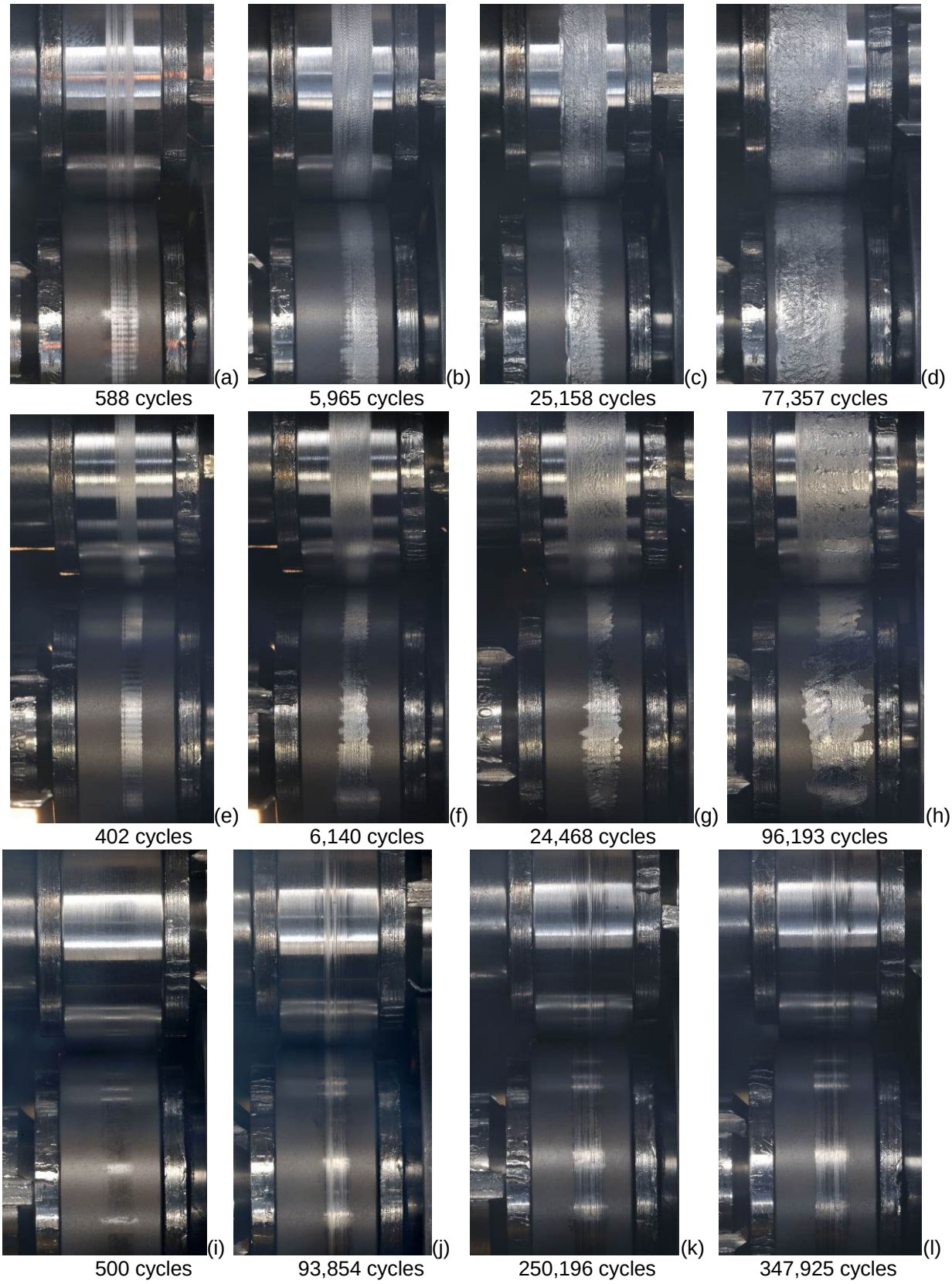

Figure 8.—Progression of wear during 3 tests. The cycle count is denoted below each photo.
(a-d) 440F at 1.4° misalignment. (e-h) 440C at 1.5° misalignment. (i-l) 440F at 0.0° misalignment.

TABLE 1.—SUMMARY OF TEST CONDITIONS

test #	roller pair	test ID	upper roller		lower roller		test conditions	
			material	outer surface condition	material	outer surface condition	speed (rpm)	misalignment angle (deg)
1	1	1	440C	bare	Ti6Al4V	bare	15	-1.4
2	2	2	440F	bare	Ti6Al4V	bare	15	-1.4
3	3	3	440F	bare	Ti6Al4V	anodized	15	-1.4
4	4	4	440F	bare	Ti6Al4V	anodized	15	0.0
5	5	5	440F	passivated	Ti6Al4V	anodized	9	-1.4
6	6	6	440F	passivated	Ti6Al4V	anodized	15	-0.4
7	7	7	440F	passivated	Ti6Al4V	anodized	15	-0.9
8	8	8(a)	440F	passivated	Ti6Al4V	anodized	15	0.0
9	8	8(b)	440F	passivated	Ti6Al4V	anodized	15	-0.1
10	8	8(c)	440F	passivated	Ti6Al4V	anodized	15	-0.2
11	8	8(d)	440F	passivated	Ti6Al4V	anodized	15	-0.3
12	8	8(e)	440F	passivated	Ti6Al4V	anodized	15	-0.7
13	9	9	440C	bare	Ti6Al4V	anodized	15	-1.5
14	10	10	440C	bare	Ti6Al4V	anodized	15	-1.4
15	11	11	440C	passivated	Ti6Al4V	anodized	15	-0.9

To study the wear, rollers were inspected using a scanning electron microscope (SEM). By using x-ray photoelectron spectroscopy the constituents of particular regions of the rollers could be investigated. In all cases, two-way transfer of material was observed. That is, titanium alloy substrate was found on the 440 steel rollers and steel alloy was found adhered to the titanium alloy rollers. An example from inspection of the titanium alloy roller from test ID 3 of Table 1 is provided in Figure 9. An overall view of a region near the center of the wear track is given in Figure 9(a), and also noted are regions where spectroscopy was assessed. The bright regions noted as #1 and #2 in Figure 9(a) produced the respective spectra of Figure 9(b) and (c). Here in the spectra of Figure 9(b) and (c) we note the clear presence of iron, chromium, and alloying elements of the 440 steel. Region #2 had a brighter appearance suggesting a more complete coverage of the substrate, and the spectrum for region #2, Figure 9(c), has a very strong peak correlating to iron. The darker region noted as numeral 3 in Figure 9(a) produced the spectrum of Figure 9(d). Here the titanium is still exposed, we observe peaks correlating to titanium and aluminum, and peaks correlating to iron and chromium are not present. The spectrum for the region marked with the numeral 4 in Figure 9(a) is not shown here but was consistent with that of Figure 9(d). These trends were true for all of many samples inspected. In all cases the worn regions included regions of the base material still exposed and also contained adhered material from the mating roller. As will be noted, in net, mass was lost for the 440 steel rollers. However, in all cases Ti6Al4V material was found on the tested steel rollers via SEM spectroscopy.

The roller masses were determined using a scale with digital readout to 0.0001 g. Masses of the rollers were measured after cleaning and just before installation in the test rig. The roller masses were also measured just after removal from the test chamber. The change in mass at the end of the test quantifies the net transfer of material by adhesive wear. The sum of the mass change for the two rollers provides a calculated value of debris lost from the roller pair. Because of practical test considerations, the test durations were not the same for each test. To provide a method for direct quantitative comparison, the change in mass was divided by the total number of revolutions of the input shaft (that is the total number of contact stress passes) to quantify the wear rate. The mass change data and calculated wear rates are summarized in Table 2.

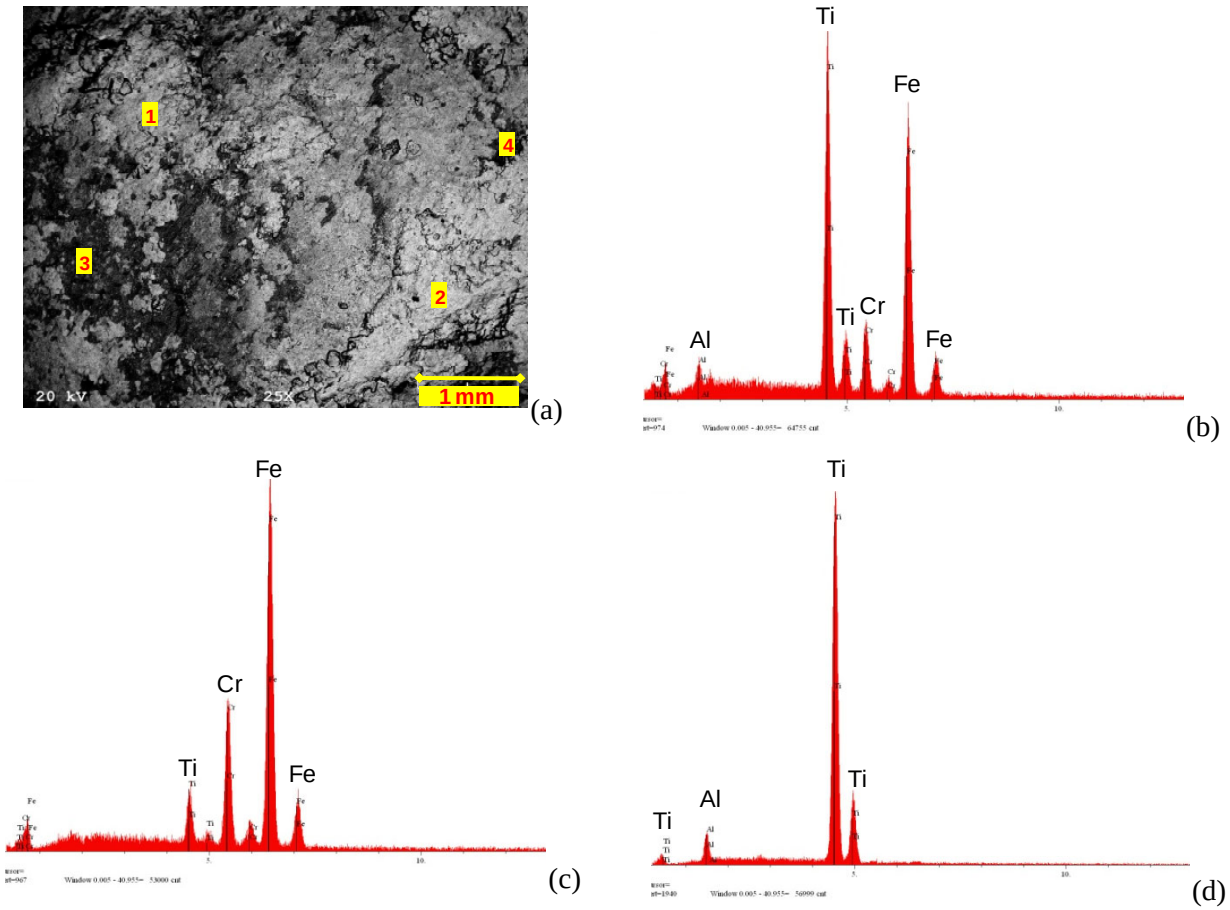

Figure 9.—Scanning electron inspections of the wear track on the titanium test roller for test #3. (a) SEM image. (b) Spectrum for region noted as 1 in 9(a). (c) Spectrum for region noted as 2 in Figure 9(a). (d) Spectrum for region noted as 3 in Figure 9(a).

TABLE 2.—SUMMARY OF ROLLER WEAR TEST RESULTS

		test duration	mass change; Ti6Al4V	mass change; 440 steel	calculated mass liberated	calculated rate of mass liberated
test #	test ID	revolutions of input shaft	grams	grams	milligrams	micrograms per cycle
1	1	26,080	0.0049	-0.0054	0.500	0.019
2	2	60,228	0.0981	-0.1258	27.700	0.460
3	3	77,326	0.1350	-0.2072	72.200	0.934
4	4	347,925	-0.0006	-0.0052	5.800	0.017
5	5	55,411	0.0817	-0.1052	23.500	0.424
6	6	60,850	0.0151	-0.0210	5.900	0.097
7	7	124,900	0.1314	-0.1664	35.000	0.280
8	8(a)	93,027	-0.0005	-0.0038	4.300	0.046
9	8(b)	24,001	0.0012	-0.0012	0.000	0.000
10	8(c)	24,000	0.0017	-0.0018	0.100	0.004
11	8(d)	24,095	0.0025	-0.0027	0.200	0.008
12	8(e)	93,117	0.0464	-0.0501	3.700	0.040
13	9	96,193	0.0682	-0.0698	1.600	0.017
14	10	41,055	0.0200	-0.0210	1.000	0.024
15	11	90,004	0.0672	-0.0688	1.600	0.018

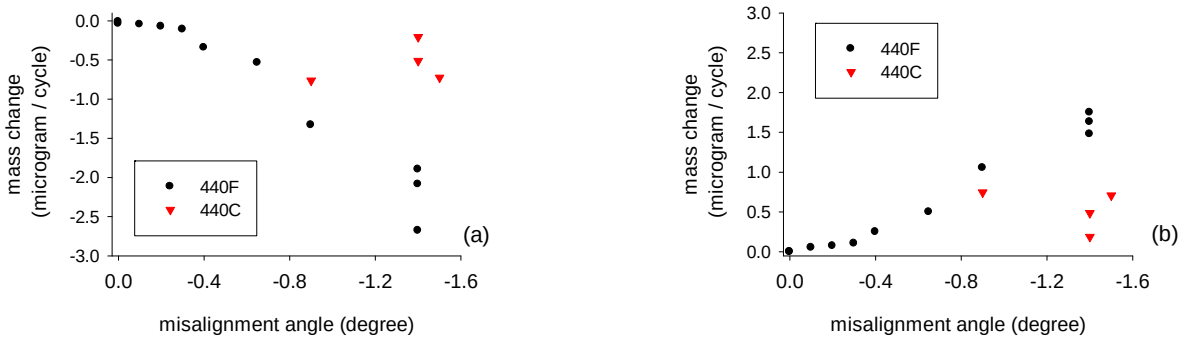

Figure 10.—Change of mass per cycle (shaft revolution) as a function of misalignment angle. (a) Mass loss of 440 steel rollers. (b) Mass increase of Ti6Al4V rollers, symbols denoting the mating material.

Often wear is modeled as proportional to the sliding distance. In these roller tests, to a first order effect the sliding distance is proportional to the misalignment angle. The rate of mass change was plotted as a function of misalignment angle (Fig. 10). Note that in the net, the steel rollers lost mass while the titanium alloy rollers gained mass. We also note that the 440F material had a higher rate of wear compared to the 440C in all cases. Rabinowicz (Ref. 8) has noted that the experimental evidence for wear rate being proportional to sliding distance (as often assumed true) is mixed. He states that usually the relationship is not perfectly obeyed but the proportional relationship represents experimental data "reasonably well". This observation matches the behavior from this investigation in that the misalignment angle (and thereby the sliding distance) correlates to the wear rate, but the linear relationship is not exact. Not only the wear rate but also the wear behavior differed for tests with 440F steel versus 440C steel. Adhesive wear tends to progress toward an "equilibrium surface" (Ref. 8) meaning the surface roughness changes with running, and the wear process can either roughen or smoothen the surfaces depending on the materials and starting conditions. The equilibrium surfaces for the tests with 440F versus 440C differed as depicted in Figure 11. Tests with the 440C material resulted in smoother running surfaces (Fig. 11(b)), and the photos suggest that the particle size of wear debris is likely smaller, in general, for the case of 440C. The Ti6Al4V rollers when mated with the 440F steel tended to gain material by adhesive wear in a more uniform fashion, that is, the coverage of the surface was more significant and uniform in appearance. It is possible that the hardened 440C behavior differed from that of the annealed 440F not only because of the change of the elastic limit but also because of an alteration of the metallurgical structure and alteration of the adhesion compatibility with the Ti6Al4V (Ref. 8).

Wear Debris

During testing of the qualification test unit, some loose debris was formed. The scope of the NESC assessment included consideration of mission risk from the loose debris. The laboratory testing revealed aspects of the loose debris as follows. From Table 2, note that loose debris was generated at rates on the order of 0.5 μg per cycle for large roller misalignment. The wear rates were greatly reduced for the case of zero roller misalignment. However, the adhesive wear was not completely eliminated with aligned rollers, and some debris was formed. Figure 12(a) and (b) provides images of the largest sized particles collected from the two tests operated with zero roller misalignment. Figure 12(c) is a typical example of the large number and widely distributed debris that occurred for extensive run time and the largest misalignment angles tested. A portion of the debris pan was not within direct line of sight of the rollers, but that region still contained significant numbers of particles.

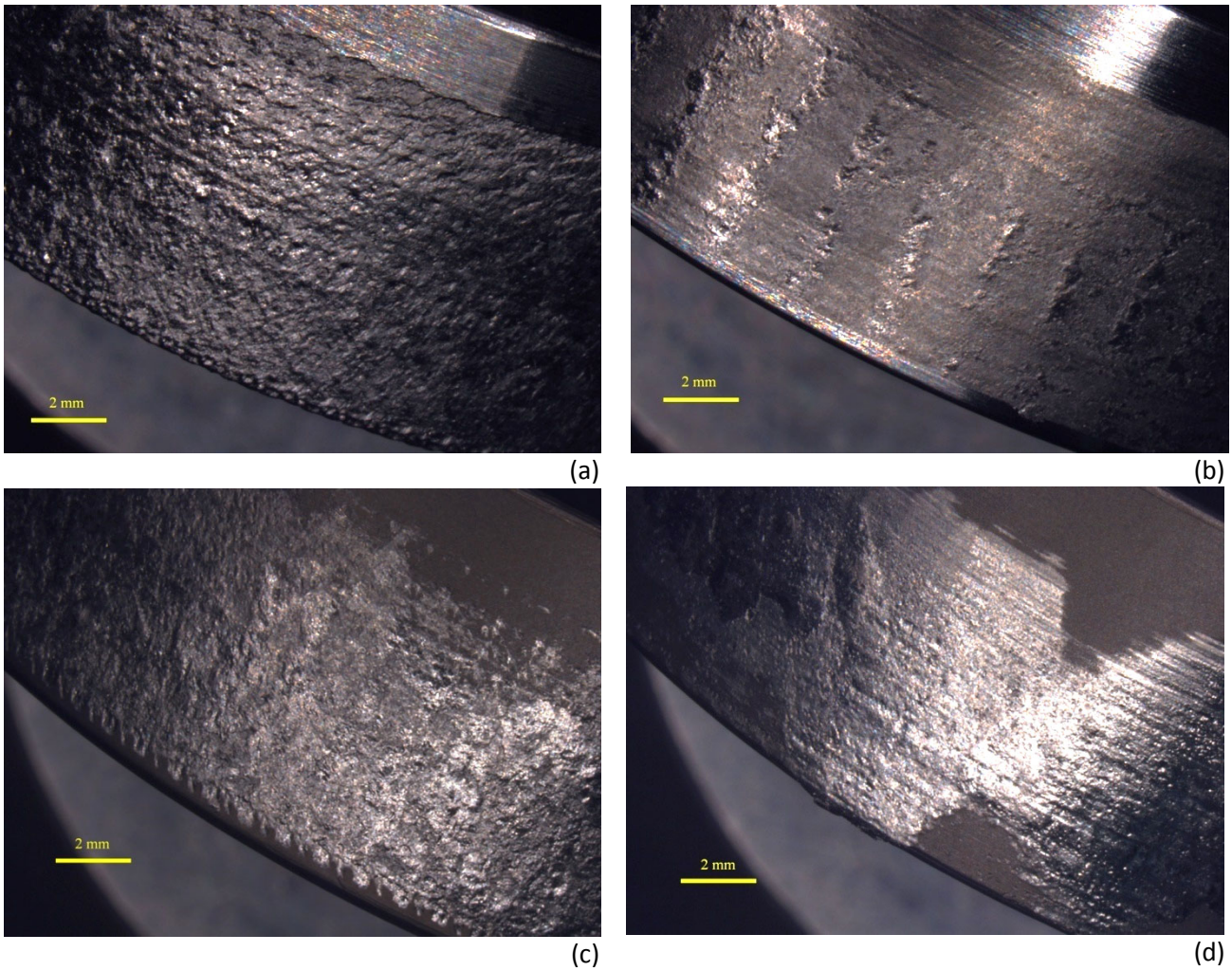

Figure 11.—Condition of rollers at end of test showing differing behavior of 440F vs. 440C. (a) 440F, test ID 5. (b) 440C, test ID 9. (c) Ti6Al4V test ID 5. (d) Ti6Al4V, test ID 9. The test ID numbers refer to Table 1.

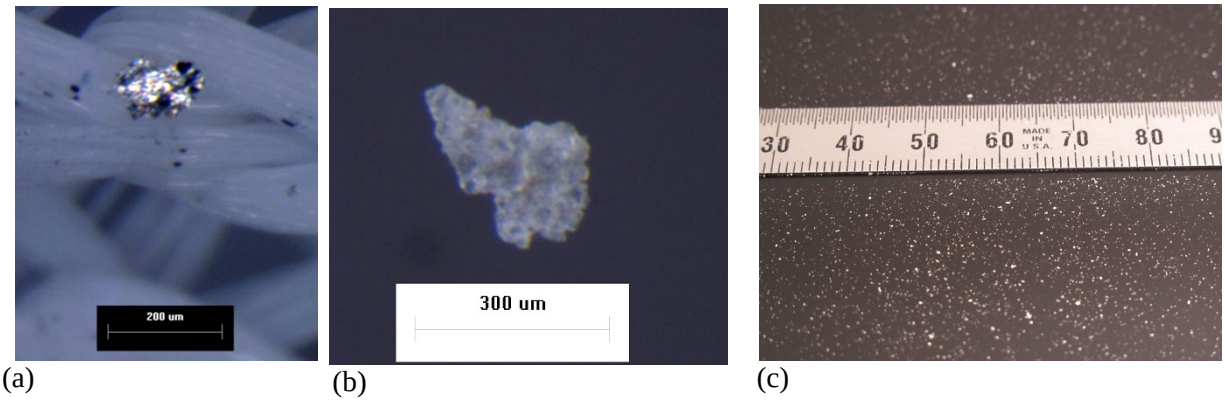

Figure 12.—Examples of loose particle debris. (a) Test ID 4 with zero roller misalignment. (b) Test ID 8(a) with zero roller misalignment. (c) Test ID 5, rollers misalignment –1.4°. The test ID numbers refer to Table 1.

Summary

Laboratory testing of 440 steel rollers in contact with Ti6Al4V in vacuum was completed to study the wear behavior and to quantify wear rates. The tests also assessed the influence of material condition and roller misalignment. The wear rate was found to be roughly proportional to the roller misalignment angle. The rate of loose particle mass created was on the order of 0.5 μg per cycle. The adhesive wear was a two-way phenomenon with titanium alloy material found adhered to the steel and vice versa. Loose particles with linear dimensions on the order of 200 μm were created even for the condition of zero roller misalignment. For large misalignment angles, large numbers of loose particles could be created, and debris was found in locations that were not within a direct line of sight. The wear behavior differed for the case of 440F and 440C steel rollers. With the 440C rollers, the adhesive wear rate was reduced, and the final surface textures of the 440C rollers were smoother than the 440F rollers.

References

1. McClendon, M., "NIRSpec MSS Magnet Actuator Life Test Unit Wear Particle Evaluation," obtained by Krantz, T., May 16, 2011.
2. Authors unstated, "Micro Shutter Subsystem (MSS) Qualification Unit Test Report," JWST-RPT-013819, Rev. A, June 2010.
3. Pepper, S., "Research Note-Characterization of the Test Environment of JWST Roller Wear Evaluation at NASA-GRC," Aug. 1, 2011.
4. Johnson, K.L., Contact Mechanics, Cambridge University Press, 1985.
5. Kalker, J.J., "Rolling contact phenomena: linear elasticity," Rolling Contact Phenomena CISM Courses and Lectures, Issue 411, Spinger-Verlag, 2000.
6. McGinness, H., "Lateral forces induced by a misaligned roller," DSN Progress Report 42-45, March and April 1978, Jet Propulsion Laboratory, Pasadena, Calif., 1978.
7. Krantz, T., DellaCorte, C., Dube, M., "Experimental Investigation of Forces Produced by Misaligned Steel Rollers," proceedings of the 40th Aerospace Mechanisms Symposium, NASA/CP—2010-216272, also NASA/TM—2010-216741, 2010.
8. Rabinowicz, E., Friction and Wear of Materials, 2nd edition, Wiley-Interscience, 1995.
9. Vijayakar, S., "A combined surface integral and finite element solution for a three-dimensional contact problem," International J. of Numerical Methods for Engineering, vol. 31, 1991.
10. Vijayakar, S., "Multi-body Dynamic Contact Analysis Tool for Transmission Design – SBIR Phase II Final Report," Army Research Laboratory ARL-CR-487, 2003.

REPORT DOCUMENTATION PAGE	Form Approved OMB No. 0704-0188

1. REPORT DATE *(DD-MM-YYYY)*	2. REPORT TYPE	3. DATES COVERED *(From - To)*
01-06-2012	Technical Memorandum	

4. TITLE AND SUBTITLE
Wear of Steel and Ti6Al4V Rollers in Vacuum

5a. CONTRACT NUMBER

5b. GRANT NUMBER

5c. PROGRAM ELEMENT NUMBER

6. AUTHOR(S)
Krantz, Timothy, L.; Shareef, Iqbal

5d. PROJECT NUMBER

5e. TASK NUMBER

5f. WORK UNIT NUMBER
WBS 869021.05.03.05.12

7. PERFORMING ORGANIZATION NAME(S) AND ADDRESS(ES)
National Aeronautics and Space Administration
John H. Glenn Research Center at Lewis Field
Cleveland, Ohio 44135-3191

8. PERFORMING ORGANIZATION REPORT NUMBER
E-18207

9. SPONSORING/MONITORING AGENCY NAME(S) AND ADDRESS(ES)
National Aeronautics and Space Administration
Washington, DC 20546-0001

10. SPONSORING/MONITOR'S ACRONYM(S)
NASA

11. SPONSORING/MONITORING REPORT NUMBER
NASA/TM-2012-217619

12. DISTRIBUTION/AVAILABILITY STATEMENT
Unclassified-Unlimited
Subject Category: 37
Available electronically at http://www.sti.nasa.gov
This publication is available from the NASA Center for AeroSpace Information, 443-757-5802

13. SUPPLEMENTARY NOTES

14. ABSTRACT
This investigation was prompted by results of a qualification test of a mechanism to be used for the James Webb Space Telescope. Post-test inspections of the qualification test article revealed some loose wear debris and wear of the steel rollers and the mating Ti6Al4V surfaces. An engineering assessment of the design and observations from the tested qualification unit suggested that roller misalignment was a controlling factor. The wear phenomena were investigated using dedicated laboratory experiments. Tests were done using a vacuum roller rig for a range of roller misalignment angles. The wear in these tests was mainly adhesive wear. The measured wear rates were highly correlated to the misalignment angle. For all tests with some roller misalignment, the steel rollers lost mass while the titanium rollers gained mass indicating strong adhesion of the steel with the titanium alloy. Inspection of the rollers revealed that the adhesive wear was a two-way process as titanium alloy was found on the steel rollers and vice versa. The qualification test unit made use of 440F steel rollers in the annealed condition. Both annealed 440F steel rollers and hardened 440C rollers were tested in the vacuum roller rig to investigate possibility to reduce wear rates and the risk of loose debris formation. The 440F and 440C rollers had differing wear behaviors with significantly lesser wear rates for the 440C. For the test condition of zero roller misalignment, the adhesive wear rates were very low, but still some loose debris was formed.

15. SUBJECT TERMS
Wear; Steel; Titanium; Tribology; Rollers

16. SECURITY CLASSIFICATION OF:			17. LIMITATION OF ABSTRACT	18. NUMBER OF PAGES	19a. NAME OF RESPONSIBLE PERSON
a. REPORT	b. ABSTRACT	c. THIS PAGE			STI Help Desk (email:help@sti.nasa.gov)
U	U	U	UU	20	19b. TELEPHONE NUMBER *(include area code)* 443-757-5802